Marine Pollution Bulletin 230 (2026) 119817

Contents lists available at ScienceDirect

Marine Pollution Bulletin

journal homepage: www.elsevier.com/locate/marpolbul

Pollution characteristics and health risks of PAHs and their nitrated and oxygenated derivatives in the ambient air of a major iron and steel industrial city in South Korea☆

Minji Go [a], Ho-Young Lee [a], Jeong-Tae Ju [a], Seongjin Hong [b], Sung-Deuk Choi [a,*]

[a] Department of Civil, Urban, Earth, and Environmental Engineering, Ulsan National Institute of Science and Technology (UNIST), Ulsan, 44919, Republic of Korea
[b] Department of Earth, Environmental & Space Sciences, Chungnam National University, Daejeon, 34134, Republic of Korea

ARTICLE INFO

Keywords:
PUF-PASs
PAHs
NPAHs
OPAHs

ABSTRACT

The levels, profiles, sources, and health risks of polycyclic aromatic hydrocarbons (PAHs), nitrated PAHs (NPAHs), and oxygenated PAHs (OPAHs) were investigated in Pohang, a major iron and steel industrial city in South Korea. Passive air samplers (PASs) were deployed at 26 sites across port, industrial, and urban areas during winter for a 72-day sampling period. The mean concentrations of 21 PAHs, 17 NPAHs, and 9 OPAHs were 54.6 ng/m^3, 530 pg/m^3, and 4.8 ng/m^3, respectively. The mean PAH concentration at the port area was 3.9 times higher than that in other areas, primarily due to emissions from steel production processes (e.g., sintering and blast furnaces) and ship and truck activities related to cargo handling. Among NPAHs, 1-nitropyrene, a marker of diesel exhaust, was predominant at the port sites, highlighting the contribution of traffic emissions. OPAHs showed a spatial distribution similar to that of PAHs, with 9-fluorenone being the most abundant compound. Correlation analysis, diagnostic ratios, and principal component analysis revealed the influence of primary emission sources, including iron and steel manufacturing, diesel exhaust, and coal combustion, as well as contributions from secondary formation. Cancer risk assessments indicated elevated health risks in the port area, with PAHs being the major contributors. Overall, PAH and N/OPAH levels were largely driven by primary emissions in the port area, while secondary formation played a more significant role in the urban areas. This study is the first in South Korea to report atmospheric levels of both NPAHs and OPAHs using PASs.

1. Introduction

Polycyclic aromatic hydrocarbons (PAHs) are organic compounds consisting of two or more fused aromatic rings. These compounds originate from both natural sources, such as wildfires and volcanic activity, and anthropogenic processes, including the combustion of petroleum and coal (Cave et al., 2018; Meng et al., 2019). Their atmospheric behavior and transformation are strongly influenced by meteorological conditions, particularly temperature, wind patterns, and photochemical processes (Choi et al., 2012; Reisen and Arey, 2005). Under sunlight and oxidizing conditions, PAHs undergo photochemical reactions that produce more reactive derivatives, such as nitrated PAHs (NPAHs) and oxygenated PAHs (OPAHs) (Tsapakis and Stephanou, 2005). NPAHs are generally formed through secondary reactions involving hydroxyl or nitrate radicals and gaseous PAHs, while OPAHs are produced by photooxidation reactions between PAHs and atmospheric oxidants (Tsapakis and Stephanou, 2005). Additionally, both NPAHs and OPAHs can be directly emitted from combustion sources (Albinet et al., 2007; Li et al., 2018). These derivatives are of particular concern due to their higher toxicity than that of their parent compounds. While PAHs require metabolic activation to exert their toxic effects, some NPAHs and OPAHs act as direct mutagens and carcinogens, thereby posing greater health risks (Bandowe and Meusel, 2017; de Oliveira Galvão et al., 2024). For example, pyrene (Pyr) is classified as Group 3 (not classifiable as to its carcinogenicity to humans) by the International Agency for Research on Cancer (IARC), whereas its nitrated derivatives, 1-nitropyrene (1-NPyr), 2-nitropyrene (2-NPyr), and 4-nitropyrene (4-NPyr), are categorized as Group 2 A (probably carcinogenic to humans) or Group 2B (possibly carcinogenic to humans) (IARC, 2010, 2013).

☆ This article is part of a Special issue entitled: 'Source Apportionment' published in Marine Pollution Bulletin.

* Corresponding author.
E-mail address: sdchoi@unist.ac.kr (S.-D. Choi).

https://doi.org/10.1016/j.marpolbul.2026.119817
Received 25 August 2025; Received in revised form 15 April 2026; Accepted 28 April 2026
Available online 30 April 2026

Previous research has contributed to understanding the pollution characteristics (Li et al., 2014; Wei et al., 2012), spatial distribution (Chen et al., 2021; Wang et al., 2022), and secondary formation pathways (Ding et al., 2019; Marquès et al., 2017) of atmospheric NPAHs and OPAHs (collectively referred to as N/OPAHs). Several studies have also assessed their potential health risks in urban and rural areas (Hong et al., 2021; Huang et al., 2014). However, most of these studies have been conducted in urban areas, where emission patterns are relatively homogeneous. In contrast, industrial areas are influenced by concentrated and diverse emission sources, with considerable emissions of PAHs and N/OPAHs from various industrial processes (Choi et al., 2012; Vuong et al., 2020). Moreover, N/OPAHs can be secondarily formed via photooxidation of precursors emitted from industrial complexes (Idowu et al., 2020; Wang et al., 2022; Wei et al., 2012), suggesting that their atmospheric behavior in industrial environments may differ substantially from that in urban areas. In particular, several studies have reported elevated levels of PAHs and N/OPAHs in areas near heavy industrial sources, such as iron and steel manufacturing facilities (Liu et al., 2019; Tutino et al., 2016). Although the contribution of industrial sources to atmospheric N/OPAH levels has been recognized, studies on these compounds in industrial areas remain limited. In South Korea, a few studies have reported OPAH concentrations associated with PM_{10} (Lee et al., 2018) and $PM_{2.5}$ (Shin et al., 2022) in urban areas such as Seoul; however, no research has yet investigated N/OPAHs in the country's industrial cities. This gap highlights the need for targeted investigations to elucidate the spatial distribution, emission sources, and associated health risks of N/OPAHs.

Pohang, a major industrial city in South Korea, is a central hub for steel manufacturing. Its industrial activities have contributed significantly to particulate pollution, posing serious environmental challenges (Ryu et al., 2023). According to the Clean Air Policy Support System (CAPSS, https://www.air.go.kr), Pohang ranked second among South Korean cities in 2022 for emissions of sulfur oxides (SO_X) and carbon monoxide (CO) from industrial processes. In addition, the city ranked within the top ten for emissions of nitrogen oxides (NO_X) and particulate matter ($PM_{2.5}$ and PM_{10}) from industrial sources. A national hazardous air pollutant (HAP) monitoring station, operated by the Ministry of Environment (MOE) of South Korea, is located at an industrial site in Pohang. Data from this station indicate that annual mean concentrations of the 16 priority PAHs designated by the United States Environmental Protection Agency (US EPA) have consistently exceeded the national mean since 2018 (MOE, 2023). Furthermore, seasonal monitoring conducted at four sites in Pohang revealed that even a residential site exhibited an annual Σ_{19} PAH concentration of 85.8 ng/m^3 in both particulate and gaseous phases, highlighting severe PAH pollution in the city (Baek et al., 2020). These findings emphasize the urgent need for comprehensive investigations into the spatial distribution, sources, and impacts of PAHs and their derivatives in Pohang.

Polyurethane foam-passive air samplers (PUF-PASs) have been widely used in studies of PAHs and their derivatives due to their suitability for deployment across various locations without requiring electrical power (Kim et al., 2023; Thang et al., 2020; Vuong et al., 2020). Compared with active air samplers, which require pumps and a continuous power supply, PUF-PASs are cost-effective and easy to operate. These advantages enable simultaneous monitoring with high spatial coverage across various areas, including industrial and urban sites, even where power infrastructure is limited. However, PAS-based methods provide time-integrated concentrations and do not capture short-term variability. In addition, sampling rates can be affected by meteorological conditions such as wind speed and temperature (He and Balasubramanian, 2010). Although numerous studies have investigated PAHs and N/OPAHs in the atmosphere (Chen et al., 2021; Li et al., 2018; Zhang et al., 2019), relatively few have employed PAS-based sampling methods (Jariyasopit et al., 2018; Wang et al., 2022). Therefore, the use of PUF-PASs is appropriate for assessing the spatial distribution of these pollutants across industrial and urban areas.

In this study, PUF-PASs were deployed across Pohang to provide spatially resolved data on PAHs and their derivatives. The objectives of this study were to investigate the influence of port and industrial emissions, characterize the spatial distribution and potential sources of PAHs and N/OPAHs, and assess the associated cancer risk to residents from port operations and steel manufacturing activities.

2. Materials and methods

2.1. Study area

Pohang is the largest iron and steel industrial city facing the East Sea in South Korea. It hosts a significant iron and steel industrial complex along with one of the leading global corporations in the industry. Information on the cargo handled and the piers at Pohang New Port is summarized in Table S1 in the Supplementary Information. Pohang New Port, a national trade port, has a handling capacity of 95,278 thousand revenue tons (RT) per year, making it one of the most prominent ports in South Korea. The urban areas of Pohang, due to their proximity to both the port and the industrial complex, are significantly influenced by industrial activities.

PUF-PASs were deployed at 26 sites across the port (P1–P8), industrial (I1–I3), and urban (U1–U15) areas of Pohang (Fig. 1). The port sites are located at the boundary of POSCO steelworks, an area primarily dedicated to ironmaking, and are likely influenced by both emissions from steel production and port-related activities. In contrast, the industrial sites are primarily associated with the production of auxiliary materials as well as the processing and handling of finished steel products. The sampling period was from January 5 to March 17, 2023 (72 days). Before sampling, the PUF disks were cleaned with acetone and n-hexane, each for 30 min. The collected PUF disks were stored in polyethylene zipper bags at −4 °C.

2.2. Chemical analysis and QA/QC

The target compounds were 21 PAHs, 17 NPAHs, and 9 OPAHs. Their abbreviations are listed in Table S2. Detailed procedures for the pretreatment and analysis of the target compounds are described in Text S1 in the Supplementary Information. In short, the retrieved PUF disks were Soxhlet extracted with n-hexane/acetone. The extracts were cleaned using activated silica gel columns for PAHs and activated silica gel/alumina columns for N/OPAHs, with n-hexane/dichloromethane as eluents. Individual internal standards for PAHs and N/OPAHs were added to the vials prior to instrumental analysis. Samples collected from the port area, which exhibited high particle loads, underwent additional pretreatment to enable quantification of target compound concentrations in the particulate phase. Detailed methods for the pretreatment of particulate target compounds are described in Text S2.

For quality assurance and quality control (QA/QC), field blanks (n = 2) and lab blanks (n = 3) were analyzed to monitor contamination during sampling and experimental procedures, respectively. The blank PUF disks were pretreated and analyzed using the same methods as those applied to the actual samples. Concentrations of target compounds detected in the blanks were subtracted from those in the samples to correct for background contamination. The mean recoveries for the PAH surrogate standards were 67%, 84%, and 98% for phenanthrene-d_{10}, chrysene-d_{12}, and perylene-d_{12}, respectively. For the N/OPAH surrogate standards, the mean recoveries were 52%, 71%, 57%, 79%, and 81% for 1-nitronaphthalene-d_7, 2-nitrofluorene-d_9, 9-nitroanthracene-d_9, 3-nitrofluoranthene-d_9, and 6-nitrochrysene-d_{11}, respectively. Method detection limits (MDLs) for each compound were calculated as 3.14 times the standard deviation of the concentrations of seven replicate spiked samples (PAHs: 20 μg/mL × 1 μL, NPAHs: 10 μg/mL × 1 μL, OPAHs: 5 μg/mL × 1 μL). Based on these experiments, the accuracy (recovery) and precision (relative standard deviation: RSD) of the entire pretreatment procedure were evaluated. The mean recoveries were

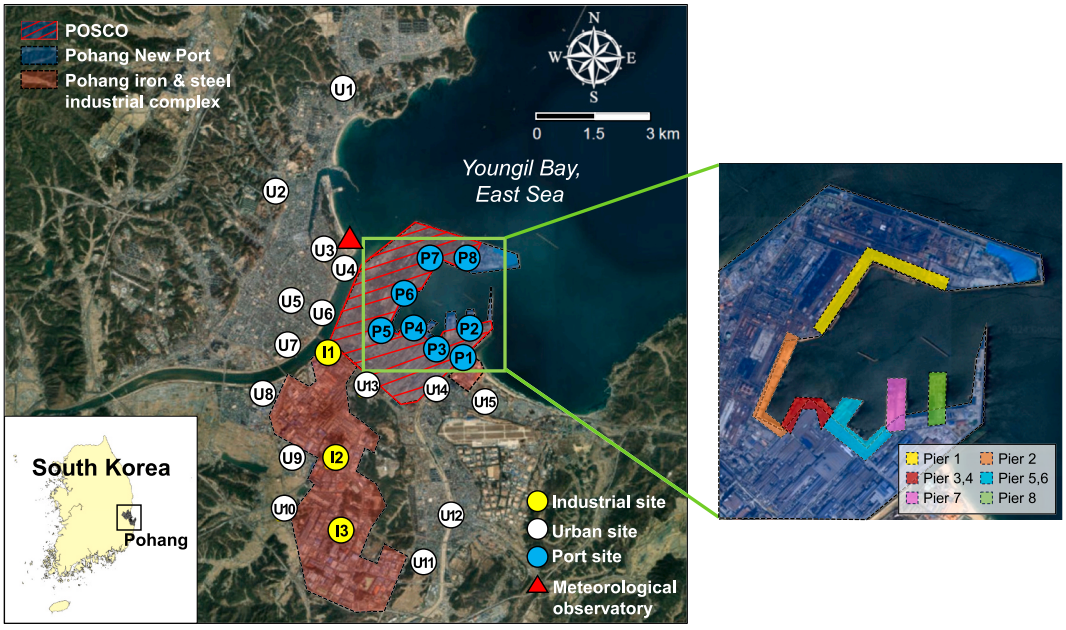

Fig. 1. Locations of 26 sampling sites and a meteorological observatory in Pohang, South Korea.

82.0%, 79.1%, and 82.4% for PAHs, NPAHs, and OPAHs, respectively, while the mean RSDs were 8.1%, 10%, and 8.4%, respectively, indicating acceptable analytical performance for the target compounds. MDLs for individual PAHs and N/OPAHs are provided in Table S3.

2.3. Meteorological conditions and calculations of air concentrations

Meteorological data for Pohang were collected from one meteorological observatory and five automatic weather stations operated by the Korea Meteorological Administration (KMA, https://data.kma.go.kr). Their detailed locations are shown in Fig. S1 in the Supplementary Information. The average wind field during the sampling period (Fig. S2) was predicted using the CALMET meteorological model within CALPUFF View (ver. 9.0, Lakes Environmental, Canada). The CALMET domain was configured with 120 × 120 horizontal grid cells at a resolution of 500 m × 500 m.

The concentrations of target compounds were calculated based on their amounts collected on PUF disks and passive sampling rates. Sampling rates for each target compound and site were estimated using a prediction model developed in a previous study, based on data from global atmospheric passive sampling networks and implemented in MATLAB. The detailed calculation method for air concentrations is described in Text S3.

2.4. Criteria air pollutant data

Criteria air pollutant (CAP) data (SO_2, CO, O_3, NO_2, PM_{10}, and $PM_{2.5}$) were obtained from 11 air quality monitoring stations (AQMSs) in Pohang via the Air Korea website (https://www.airkorea.or.kr) (Fig. S1). These CAP data were used in correlation analyses to examine their relationships with N/OPAH concentrations. The concentrations from the 11 AQMSs were interpolated using the inverse distance weighting (IDW) method in ArcGIS 10.4.1 (ESRI Inc., USA). The interpolated CAP concentrations at each sampling site were then used as input data for further analysis.

2.5. Risk assessment

The potential cancer risk associated with inhalation exposure to PAHs and NPAHs was assessed. A total of 19 PAHs and 8 NPAHs among the target compounds were selected for the evaluation. BaP equivalent (BaP_{eq}) concentrations were calculated using the toxic equivalency factors (TEFs), and the inhalation unit risk of BaP was applied to estimate cancer risk. A full description of the risk assessment is provided in Text S4.

2.6. Statistical analysis

Pearson and Spearman correlation analyses, along with Shapiro-Wilk normality tests, were performed using SPSS Statistics 25.0 (IBM, USA) to examine the relationships between PAH and N/OPAH concentrations and CAP levels. Mann-Whitney rank sum tests were conducted using SigmaPlot 12.0 (Systat Software Inc., USA). Receiver operating characteristic (ROC) analysis was implemented in Python (version 3.11) using the scikit-learn package, and the optimal threshold was determined based on Youden's index. Principal component analysis (PCA) was conducted using OriginPro 2020 (OriginLab Inc., USA) for source identification.

3. Results and discussion

3.1. Levels and profiles of PAHs and N/OPAHs

PUF-PASs are known for their effectiveness in collecting gaseous compounds and can also capture particulate compounds to some extent (Harner et al., 2013; Shoeib and Harner, 2002). Notably, samples collected from the port exhibited significant amounts of PM-bound pollutants (6.6–38.5%) on the PUF (Fig. S3). Specifically, samples (P6–P8) collected from Pier 1, where iron ore and coal are handled, contained large quantities of particulate organic compounds. Consequently, particulate PAH concentrations were calculated for all port sites except P1 and P7, where extra PUFs were unavailable. Therefore, all subsequent results and discussions address total concentrations, encompassing both particulate and gaseous phases. A detailed description of the concentrations of target compounds in PM at the port sites is provided in Text S5.

A total of 17 target PAHs, excluding DMBA, 3MCA, DahP, and DalP, were detected (Table S6). Among the 17 PAHs, DaiP was exclusively detected in the port samples, while the other PAHs were found in over 90% of the samples. Detection frequencies for 16 NPAHs ranged from

8% to 100%, while 1,8-DNP was not detected. For OPAHs, all compounds were detected in all samples except BaAD. Lower detection frequencies were observed for compounds with higher molecular weights, reflecting the greater efficiency of PUF-PAS in collecting semi-volatile compounds (Shoeib and Harner, 2002). Notably, the detected high molecular weight (HMW) PAHs and NPAHs were primarily found in the port samples, where particle loads were elevated. Other heavy compounds were generally undetected, likely due to their extremely low ambient concentrations, even under particle-rich conditions.

The mean concentration of 21 PAHs was 54.6 ng/m^3, significantly higher than the mean concentrations of NPAHs (530 pg/m^3) and OPAHs (4.8 ng/m^3). The most abundant PAH was Phe, contributing 36% of the total mean PAH concentration (Fig. 2a), followed by Flt (26%), Pyr (25%), and Flu (7%). These findings are consistent with those reported in a previous study in Ulsan using PASs (Vuong et al., 2020). Low molecular weight (LMW) PAHs tend to exist in the gaseous phase, while HMW PAHs are predominantly found in the particulate phase (Zhang et al., 2020). Therefore, the high abundance of LMW PAHs observed in this study can be explained by their gas/particle partitioning behavior (Nguyen et al., 2020). For NPAHs, 1-NPyr was the predominant compound, primarily due to its exceptionally high mean concentrations at the port sites (1.1 ng/m^3), compared with the much lower levels at the urban and industrial sites (0.02 ng/m^3) (Fig. 2b). At the urban and industrial sites, the predominant NPAHs were 1-NNap (24%), 2-NNap

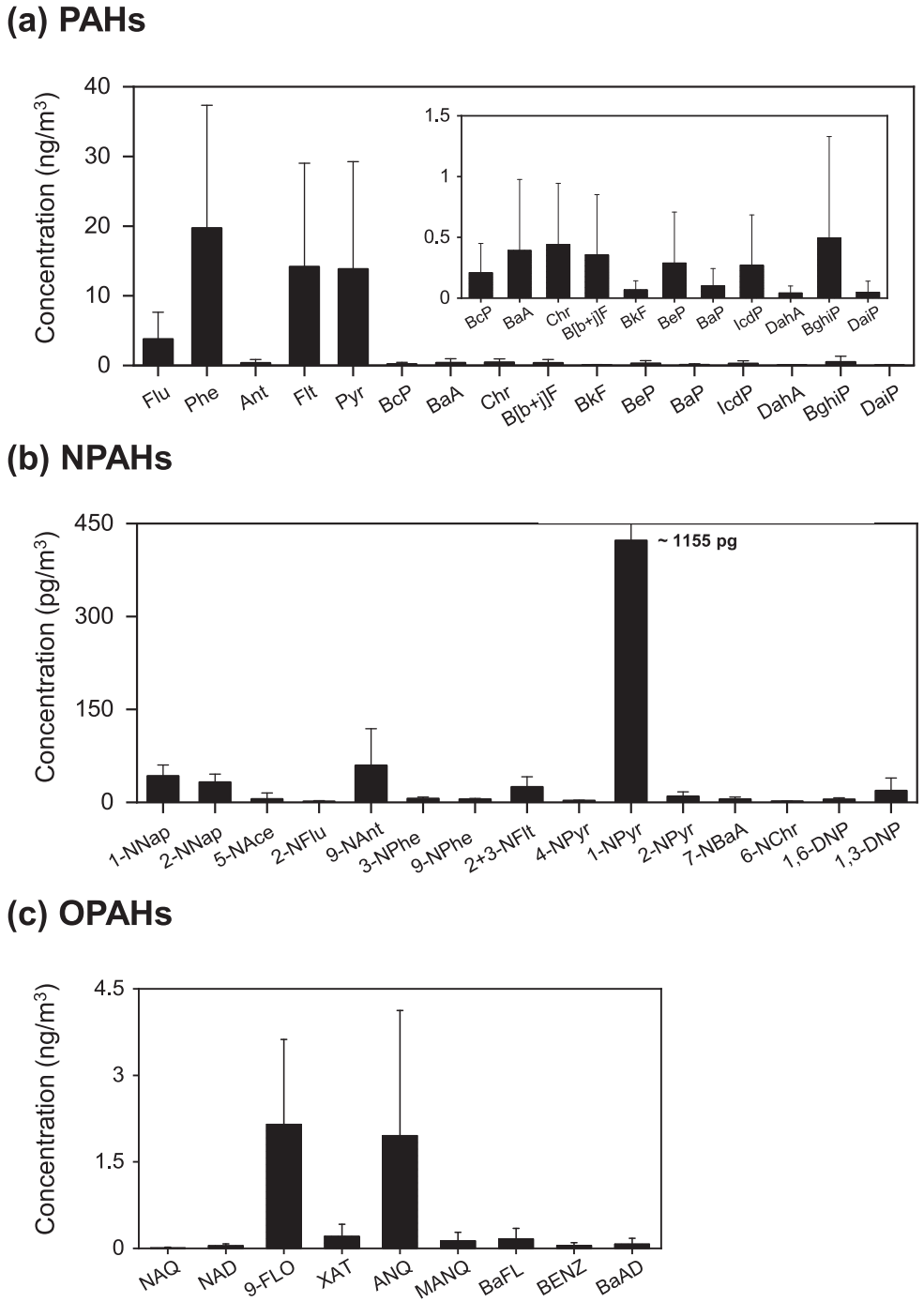

Fig. 2. Mean concentrations of (a) PAHs, (b) NPAHs, and (c) OPAHs during the sampling period (January 5–March 17, 2023) across 26 sampling sites in Pohang, South Korea.

(18%), and 9-NAnt (18%), which are consistent with previous studies (Albinet et al., 2007; Liu et al., 2017), suggesting different sources of NPAHs between the port and urban/industrial areas. For OPAHs, 9-FLO (45%) and ANQ (41%) were the most abundant compounds (Fig. 2c), in line with findings from previous studies (Albinet et al., 2007; Li et al., 2018; Wang et al., 2017). Gaseous PAHs are rapidly degraded by photolysis (Marquès et al., 2017), and the relatively low mean concentrations of Ant (0.4 ng/m^3) and Flu (3.8 ng/m^3) might contribute to the rapid formation of their derivatives such as ANQ (2.0 ng/m^3) and 9-FLO (2.2 ng/m^3).

The mean concentrations of PAHs and N/OPAHs in this study were compared with cold-season monitoring data from other cities and regions worldwide (Table S7). Due to variations in target compounds, sampling periods, and locations, this comparison provides only an approximate assessment. Overall, the PAH levels (54.6 ng/m^3) in this study were higher than those in urban areas such as Seoul, Korea (9.2 ng/m^3), and Ningbo, China (29.4 ng/m^3), but lower than those in industrial areas like Dongjiakou, China (94.9 ng/m^3). The NPAH levels in Pohang were higher than in other cities, and the OPAH levels were notably high among studies focused on gaseous concentrations. These differences are likely attributable to specific emission sources from the port and steelworks identified in this study, as well as local meteorological conditions.

The fractions of PAHs and their derivatives, classified by the number of rings at each sampling site, are presented in Fig. 3. Compounds with 3 and 4 rings constituted over 98% of the total PAHs at all sampling sites (Fig. 3a). Notably, PAH profiles differed between the port sites (P1–P6) and the urban/industrial sites. At sites P1–P6, 3-ring PAHs constituted 37% of Σ_{21} PAHs, while 4-ring PAHs accounted for 60%. In contrast, the other areas showed a different pattern, with 3-ring PAHs comprising 55% and 4-ring PAHs accounting for 44% of Σ_{21} PAHs. Furthermore, the mean fraction of 6-ring PAHs in the port was 2.4 times higher than in the other areas. These results suggest that particulate pollution is dominant in the port, as heavier compounds tend to partition into particles, reflecting the predominance of particulate emissions. The proportion of the major compound, Phe, was higher in the urban areas (45%) than in the port area (41%), while Flt was similarly distributed across all sampling sites (Fig. S4d). Additionally, Pyr accounted for a higher fraction of Σ_{21} PAHs in the port area (21%) than in the urban areas (18%), potentially contributing more significantly to the secondary formation of NPAHs.

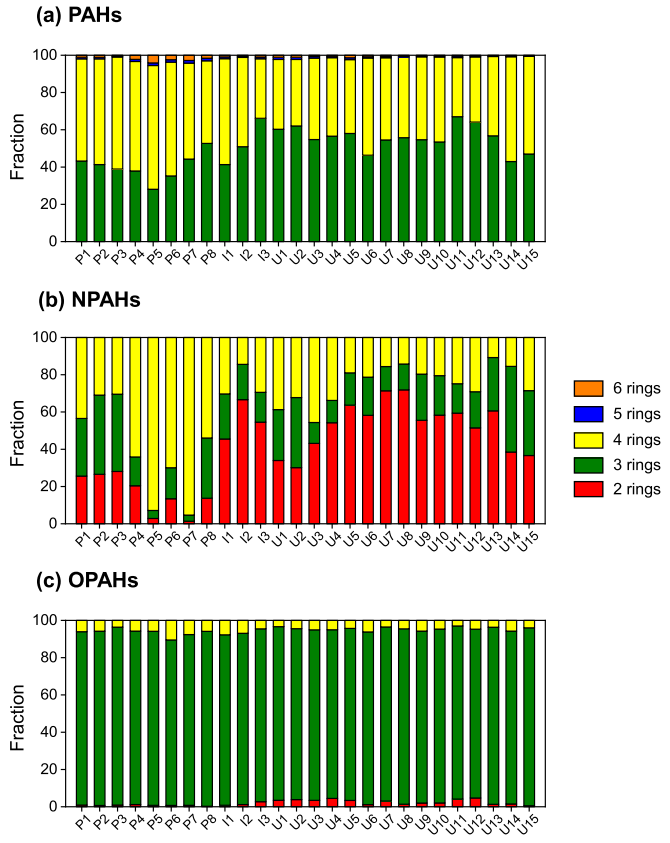

Fig. 3. Fractions of PAHs, NPAHs, and OPAHs classified by the number of rings at sampling sites.

For NPAHs, clear differences in fractions were observed between the port and non-port areas. In the port, 4-ring NPAHs constituted 65% of Σ_{17} NPAHs, while in the other areas, 2-ring NPAHs were most abundant (53%) (Fig. 3b). In non-port areas, two Nap derivatives (1-NNap and 2-NNap) accounted for mean contributions of 30% and 23%, respectively, compared with only 8% and 6% in the port. Conversely, 1-NPyr comprised 48% of Σ_{17} NPAHs in the port, but only 6% in the other areas (Fig. S4e). Since 1-NPyr is a marker for diesel engine exhaust (Teixeira et al., 2011), this result suggests significant contributions from diesel emissions originating from ships and heavy-duty trucks in the port. Specifically, sites P7 and P5, which were located at Piers 1 and 2, respectively, showed the highest proportions of 1-NPyr (94% and 88%, respectively) among all sites. This result is likely due to intensive ship and truck emissions associated with iron ore handling, particularly at Pier 1, which has the highest unloading capacity among the port sites. At sites P1–P3, 9-NAnt accounted for 34% of Σ_{17} NPAHs. Similar profiles were observed at urban sites U14 and U15, where 9-NAnt contributed 28%, notably higher than the overall urban mean of 19%. The elevated contributions of 9-NAnt at sites P1–P3 and U14–U15 are likely influenced by proximity to the industrial complex east of the port, which is primarily engaged in steel production. Notably, 9-NAnt is an indicator of coal and biomass combustion (Zhuo et al., 2017), suggesting influence from steelmaking activities involving blast furnace operations and coke combustion.

Regarding OPAH profiles, compounds with 2 rings accounted for a mean of 2%, while those with 3 rings comprised 93% of Σ_9 OPAHs (Fig. 3c). Two compounds, 9-FLO and ANQ, accounted for a mean of 86% of Σ_9 OPAHs across all sampling sites (Fig. S4f). The proportion of 9-FLO was higher in the urban and industrial areas (61%) than in the port area (34%). Conversely, ANQ contributed 51% in the port area and 25% in the other areas. 9-FLO is primarily emitted from solid fuel combustion (Li et al., 2018), whereas ANQ mainly originates from automobile exhaust (Wei et al., 2023). Consequently, OPAHs in the urban and industrial areas are predominantly from combustion sources, while in the port area, emissions from ships and trucks are the main contributors. The OPAH profiles at sites U13 and U14, with mean contributions of 47% for 9-FLO and 41% for ANQ, appear to be influenced by elevated levels at sites P1–P4, combined with the effect of westerly winds. Compounds with 4 rings contributed a mean of 5% of total OPAHs across all sampling sites, with no significant differences between port and non-port areas.

3.2. Spatial distribution of PAHs and N/OPAHs

The mean concentrations of PAHs (112 ± 44 ng/m^3), NPAHs (1423 ± 1737 pg/m^3), and OPAHs (8.3 ± 3.4 ng/m^3) at the port sites were significantly higher than those at the urban sites (PAHs: 29 ± 37 ng/m^3; NPAHs: 141 ± 88 pg/m^3; OPAHs: 3.2 ± 3.3 ng/m^3) (Mann-Whitney rank sum test, $p < 0.01$). The port sites also showed elevated PAH and NPAH levels compared with the industrial sites (PAHs: 29 ± 17 ng/m^3; NPAHs: 128 ± 60 pg/m^3) (Mann-Whitney rank sum test, $p < 0.05$). However, no statistically significant difference was observed for OPAH levels between the port and industrial sites (3.6 ± 2.5 ng/m^3) (Mann-Whitney rank sum test, $p > 0.05$). Similarly, no significant differences in PAH and N/OPAH levels were found between the industrial and urban sites, possibly due to the influence of emissions from the port and industrial areas, as most urban sites were located near these sources.

The spatial distributions of PAHs and N/OPAHs are presented in Fig. 4. The highest PAH concentration was recorded at site P6, located at Pier 1, followed by site U14 and site P8 at Pier 1. The handling of iron ore and coal cargo at Pier 1 likely contributed to these elevated levels through the dispersal of pulverized coal from cargo yards and heavy vehicle emissions. Site P6 was also heavily influenced by coal-handling operations related to coke production, sintering, and blast furnace processes from steelworks near Pier 2. Additionally, site P1, situated on the periphery of Pohang New Port, showed a high PAH concentration. This spatial distribution is closely linked to prevailing westerly winds during winter, which transport pollutants from the adjacent steel industrial complex and ship operations at sites P4–P6 toward site P1. OPAHs exhibited a spatial pattern similar to that of PAHs, with notably high concentrations at sites P6, U14, P8, and P1. This spatial agreement indicates a strong correlation between PAHs and OPAHs, suggesting shared emission sources. In contrast, NPAHs showed a distinct spatial distribution, with elevated concentrations at site P7 on Pier 1 and site P5 on Pier 2. The high NPAH level at site P7 may be attributed to heavy traffic, as Pier 1 serves as a hub for numerous vehicles and ships transporting iron ore.

In the industrial area, the highest PAH concentration was recorded at site I2, while site I3 exhibited the lowest level. N/OPAHs were most abundant at site I1, which is likely influenced by emissions from both the steelworks near the port area and the industrial complex. In contrast, the concentrations of PAHs, NPAHs, and OPAHs at site I3 were 3.2, 1.9, and 3.9 times lower, respectively, than the mean values for the industrial sites, indicating relatively lower industrial impact in the southern section of the industrial complex. Among the urban sites, site U14 exhibited the highest concentrations of PAHs and N/OPAHs. These elevated concentrations were primarily attributed to its proximity to the port and industrial areas. In addition, the higher wind speeds of the prevailing westerlies during winter likely enhanced pollutant transport from these emission sources to the site. Elevated levels were also observed at sites U13 and U15, which were similarly affected by the prevailing westerly winds. At sites U8–U12, located closer to the industrial complex, the mean concentrations of PAHs and OPAHs at the southwestern sites (U8–U10) were 2.0 and 1.8 times higher, respectively, than those at the southeastern sites (U11 and U12). However, NPAH concentrations were similar between these two groups, suggesting that local sources, such as open burning of agricultural residues, rather than seasonal wind patterns, contributed to the elevated PAH and OPAH levels. NPAHs appeared to be influenced by different pollution sources. Overall, the highest concentrations of PAHs and their derivatives were observed near the port area, indicating the substantial impact of the port and steelwork emissions on urban air quality. However, further investigation is required to identify specific sources and elucidate formation mechanisms.

The total emissions of NO_X, SO_X, PM_{10}, and $PM_{2.5}$ in Pohang for 2023 were obtained from CAPSS, which includes emissions from point sources (e.g., industrial combustion), area sources (e.g., industrial activities), and mobile sources (e.g., motorbikes, cars, trucks, buses, ships, and aircraft) (Kim et al., 2021). Maritime emissions were also included to assess ship contributions. The highest NO_X and SO_X emissions were observed near site U13, which is located close to the port, the industrial complex, and a major roadway with heavy traffic (Figs. S5a and b). This result suggests a strong influence from both industrial combustion and vehicular emissions. Elevated SO_X emissions in the port area further suggest an influence from steelmaking activities. Maritime SO_X emissions were also slightly elevated in the central port area. High SO_X emissions were observed at site I3, which did not match the spatial pattern of PAHs and their derivatives. This discrepancy is likely due to a steelmaking facility adjacent to site I3 that did not significantly influence PAH and N/OPAH levels during the sampling period. At sites U14 and U15, located near the eastern port and the industrial complex, NO_X and SO_X emissions were also significantly high, likely due to emissions from steelworks-related activities.

In addition, PM_{10} and $PM_{2.5}$ emissions were high near sites U13 to U15, and their spatial distribution closely matched the patterns of PAHs

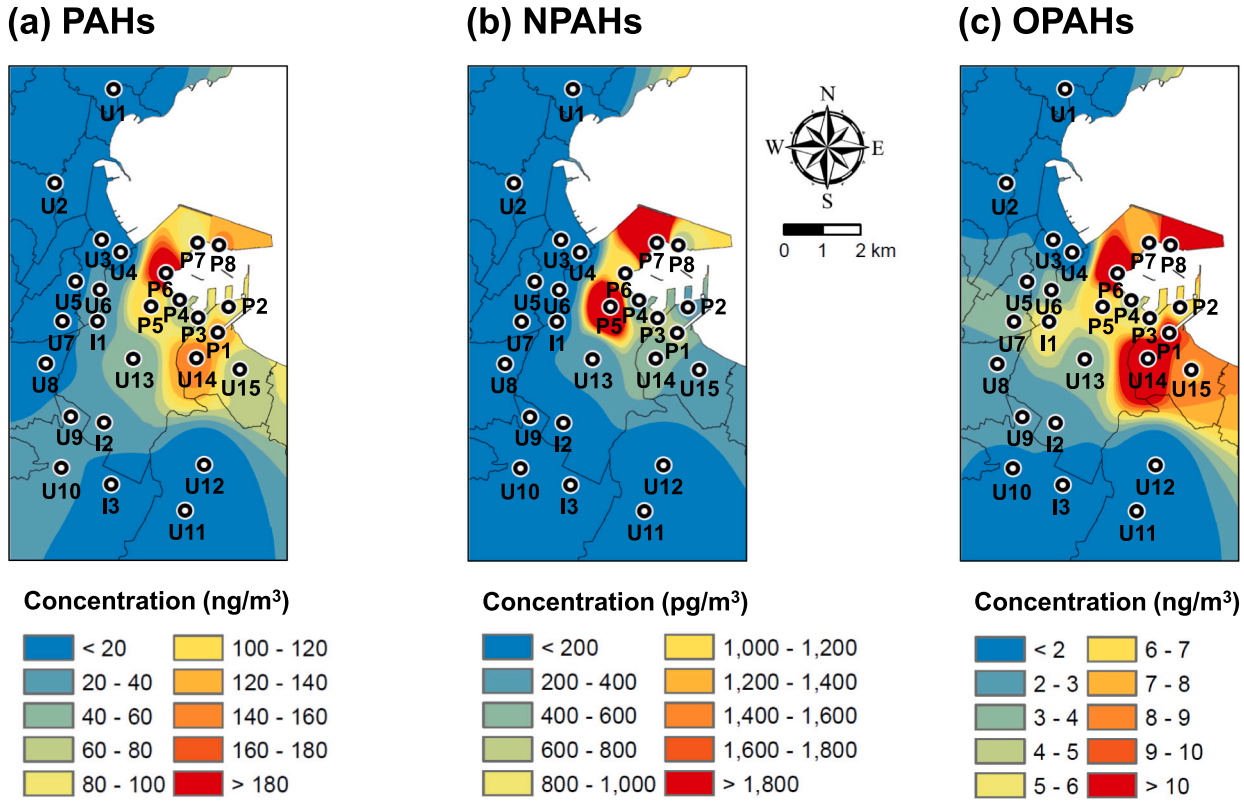

Fig. 4. Spatial distributions of Σ_{21} PAHs, Σ_{17} NPAHs, and Σ_{9} OPAHs during the sampling period. The maps were drawn using ArcGIS 10.4.1 with IDW interpolation.

and N/OPAHs observed in the urban areas (Figs. S5c and d), suggesting that these pollutants may share common sources. These findings imply that PAHs and their derivatives are likely present in ambient air via adsorption onto PM, especially under the influence of industrial and vehicular emissions. Nevertheless, emissions in the port area were relatively low compared with those in the urban areas, possibly due to the underestimation of area source emissions (e.g., sintering and blast furnace processes) and mobile sources (e.g., ship and heavy-duty truck emissions) in the CAPSS inventory.

3.3. Source identification

3.3.1. Correlation between PAHs and their derivatives

Correlation analysis revealed significant positive relationships among Σ_{21} PAHs, Σ_{17} NPAHs, and Σ_9 OPAHs ($p < 0.01$), as well as with primary air pollutants (e.g., SO_2, CO, and PM), suggesting shared emission sources and similar atmospheric behavior. Detailed results are provided in Text S6 and Tables S8–S11.

3.3.2. Assessment of secondary formation contributions to N/OPAHs

To distinguish between the contributions of primary emissions and secondary formation to N/OPAH concentrations, diagnostic ratios were calculated (Table S12). The ratio of 2-NFlt/1-NPyr was used to assess the relative influence of these sources (Huang et al., 2014; Zhang et al., 2019), where 2-NFlt serves as a marker of secondary formation (Arey et al., 1986; Liu et al., 2017), whereas 1-NPyr represents direct vehicular emissions. A higher 2-NFlt/1-NPyr ratio suggests a greater contribution from secondary formation, with values below 5 indicating primary emission dominance and values above 5 indicating secondary formation (Ciccioli et al., 1996). Although 2-NFlt and 3-NFlt could not be separated, the 2 + 3-NFlt/1-NPyr ratio was used, assuming that the atmospheric concentration of 3-NFlt is negligible compared with that of 2-NFlt (Zhang et al., 2019). This ratio was below 5 at all sites except U3, indicating the predominance of primary emissions. The mean ratios at the port, industrial, and urban sites were 0.24, 1.65, and 2.48, respectively, suggesting a relatively greater contribution of secondary formation in the urban areas, while primary emissions dominated at the port sites. Compared with a winter PAS-based study (Wang et al., 2022), reporting a mean ratio of 3.99, the lower ratios observed at the port sites in this study further support the dominance of direct emissions. Secondary formation pathways were also evaluated using the 2-NFlt/2-NPyr ratio, where values near 10 and above 100 indicate daytime OH radical- and nighttime NO_3 radical-initiated reactions, respectively (Albinet et al., 2007; Arey et al., 1986; Zhang et al., 2019). In this study, all sites exhibited 2 + 3-NFlt/2-NPyr ratios below 10, implying that secondary formation of NPAHs was primarily driven by daytime OH radical reactions.

The 9-FLO/1-NPyr ratio was used as an indicator of secondary formation, representing the relationship between the most abundant secondary OPAH (9-FLO) and the dominant primary NPAH (1-NPyr) (Ding et al., 2019). This ratio was significantly lower at the port sites than at the industrial sites (Mann-Whitney rank sum test, $p < 0.05$) and the urban sites ($p < 0.01$), while no significant difference was found between the industrial and urban sites ($p > 0.05$). To determine an appropriate threshold for distinguishing the port area from the non-port areas, an ROC analysis was conducted using data from 8 port sites and 13 non-port sites. The area under the curve (AUC) was 0.99 ($p < 0.001$), indicating excellent discriminatory power. The optimal threshold ratio, determined at a true positive rate (TPR) of 0.92 and a false positive rate (FPR) of 0.00, was 102. Accordingly, a 9-FLO/1-NPyr ratio greater than 102 is proposed as an indicator of the predominance of secondary formation over primary emissions. The mean ratio at the port sites (17.8) was 11.5 times lower than that at the non-port sites (206), supporting the validity of this threshold. Reported ratios from previous studies were also consistent with this threshold: 273 in urban areas (Albinet et al., 2007) and 89.0 in an industrial area (Wang et al., 2022).

To further assess secondary formation, the ratios of NPAHs and OPAHs to their corresponding parent PAHs were calculated. Among these ratios, five NPAH and four OPAH ratios showed statistically significant differences between the port and non-port areas (Fig. S6). For NPAHs, the mean ratios of 2-NFlu, 2 + 3-NFlt, 2-NPyr, and 7-NBaA to their parent PAHs were significantly lower in the port area ($p < 0.05$), indicating enhanced secondary formation in the industrial and urban areas. Conversely, the mean 1-NPyr/Pyr ratio was significantly higher in the port area ($p < 0.01$), suggesting a stronger influence from diesel emissions and coal combustion (Tang et al., 2011; Zhang et al., 2019). The mean ratio at the non-port sites (0.002) was consistent with values reported for coal combustion in a previous study (Tang et al., 2005). In contrast, the higher ratio at the port sites (0.04) suggests contributions from diesel emissions (e.g., trucks and ships) as well as steel-related industries (Li et al., 2014; Tang et al., 2005). Notably, site P7 showed a ratio of 0.21, suggesting a strong influence from vehicle exhaust at Pier 1.

For OPAHs, the ratios of 9-FLO, XAT, ANQ, and BaAD to their parent PAHs were significantly lower at the port sites ($p < 0.05$), further supporting the dominance of direct emissions of parent PAHs in the port area. Previous studies have reported 9-FLO/Flu, ANQ/Ant, and BaAD/BaA ratios for various sources: 0.40, 0.89, and 0.16 for crop residue combustion; 0.25, 0.14, and 0.03 for coal combustion (Shen et al., 2013); 2.06, 0.79, and 0.07 for fuelwood combustion (Shen et al., 2011; Shen et al., 2012); and 2.7, 7.7, and 0.65 for urban areas (Wang et al., 2017) (Fig. S7). In this study, the mean 9-FLO/Flu ratio was 0.42 at the port and 0.91 at the non-port sites. The lowest ratio (0.18) was observed at site P8, while the highest (1.6) was recorded at site I1. These findings indicate that the port area was dominated by freshly emitted PAHs from coal combustion. In contrast, the higher ratios at the industrial and urban sites may reflect additional contributions from secondary formation or biomass burning, likely originating from croplands southwest of the industrial complex and transported by the prevailing westerly winds. The mean ANQ/Ant ratio was 5.0 in the port area and 7.2 elsewhere, indicating more pronounced secondary formation in the urban areas. Similarly, the mean BaAD/BaA ratio was 0.18 in the port and 0.3 in other areas, consistent with the presence of fresher combustion-related emissions in the port area. For the XAT/Ant ratio, a mean value of 0.48 was observed at the port sites, compared with 1.6 in the urban areas, again suggesting more extensive PAH oxidation where direct emissions were less dominant.

It should be noted that these observations are based on a winter sampling campaign, a period typically dominated by primary combustion emissions. During summer, the contribution of secondary formation may increase due to enhanced photochemical activity, even in industrial port areas such as Pohang. Although industrial sources exert a strong influence throughout the year, the atmospheric behavior and transformation pathways of N/OPAHs may vary considerably by season. Therefore, long-term monitoring across multiple seasons is required to characterize annual trends and to provide a more comprehensive assessment of secondary formation in this area.

3.3.3. PCA results

The first three principal components (PCs), each with an eigenvalue >1, explained 68.5% of the total variance, which was sufficient to support the identification of sources of PAHs and their derivatives (Fig. 5). IcdP and BghiP, known markers of coke and coal combustion (US EPA, 1995), were associated with samples from sites P4 to P8, indicating a strong influence from iron and steel production activities west of the port. These compounds are also linked to automobile emissions (Lim et al., 1999; Liu et al., 2017), suggesting additional contributions from ship traffic and heavy-duty trucks used to transport iron and ore. Additionally, HMW PAHs, such as BaA and B[b + j]F, were prevalent at the port sites, supporting the influence of PM emissions from steel-related activities. In contrast, naphthalene derivatives (1-NNap and 2-NNap) and 2-NPyr, which are likely produced via secondary

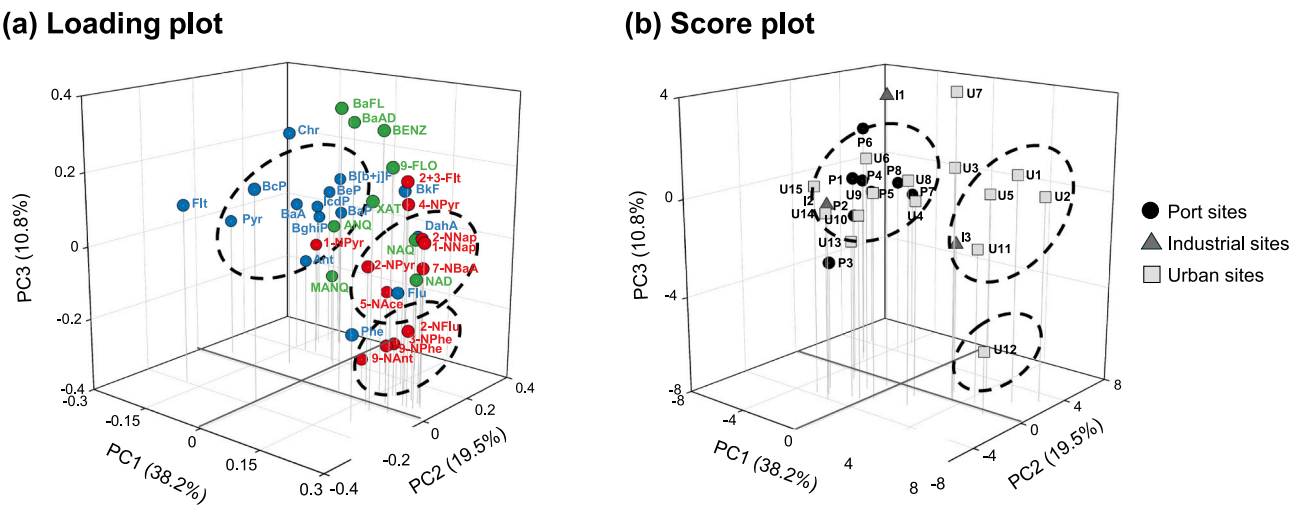

Fig. 5. PCA results for each sampling site: (a) loading plot and (b) score plot.

formation (Wei et al., 2012), were dominant at the urban sites (e.g., U1, U2, U5, and U11). Site U12 was characterized by elevated fractions of NPAHs, particularly 9-NAnt and 2-NFlu, found at high concentrations in emissions from heavy-duty diesel engines (Nagato, 2018). This finding suggests that site U12 was heavily influenced by traffic emissions from a major roadway connecting the port and the industrial complex to nearby urban areas.

PC1 explained 38.2% of the total variance. Variables with high loadings on PC1 (> 0.2), including 1-NNap, 2-NNap, 2-NFlu, 2 + 3-NFlt, 7-NBaA, NAQ, NAD, and 9-FLO, were strongly associated with secondary formation. While most variables showed strong correlations ($r > 0.7$, $p < 0.01$), NAQ and NAD exhibited weaker correlations with other compounds, which may reflect their high reactivity and rapid atmospheric degradation under sunlight (McWhinney et al., 2013; Sari Doré et al., 2025). The presence of 2 + 3-NFlt reflects secondary formation, and compounds such as 1-NNap, 2-NNap, and 9-FLO can serve as tracers for NPAHs formed through secondary reactions (Wang et al., 2022). PC1 scores were lower at the port sites than at the industrial and urban sites ($p < 0.05$) (Fig. S8a), with the higher scores observed at the urban sites (U1, U2, U11, and U12), indicating that N/OPAH concentrations in these areas were predominantly influenced by secondary formation rather than primary emissions. These findings suggest elevated health risks in densely populated urban areas west of the port, especially during summer, when prevailing northeasterly winds and enhanced photochemical activity contribute to increased pollutant levels.

PC2 (19.5% of the total variance) represented primary emissions, with high loadings (> 0.3) for B[b + j]F, BeP, BaP, IcdP, DahA, and BghiP. DahA and BghiP are primarily released from iron and steel plants (Wang et al., 2022), while B[b + j]F and IcdP are well-known indicators of vehicle exhaust (Liu et al., 2017). The port sites exhibited higher PC2 scores than the industrial and urban sites ($p < 0.05$), particularly at western port sites (P5, P7, and P8) (Fig. S8b). These results suggest that primary emissions dominate in the port area, mainly from iron ore and coal handling, as well as ship and truck traffic at Piers 1 and 2. A previous study has reported elevated PM emissions during the sintering process in iron and steel plants (Jia et al., 2018), further supporting the role of industrial activities in elevating levels of PAHs and their derivatives in the port area.

PC3 (10.8% of the total variance) was characterized by high loadings (> 0.3) for 4-ring OPAHs, including BaFL, BENZ, and BaAD. While BaFL and BENZ are associated with vehicle emissions (Albinet et al., 2007; Chen et al., 2021; Ringuet et al., 2012), BaAD is indicative of secondary formation (Wang et al., 2022). No statistically significant differences in PC3 scores were observed among the three sampling groups ($p > 0.05$) (Fig. S8c), indicating that the sources represented by PC3, including traffic emissions and secondary formation, were uniformly distributed across the Pohang area. However, because PC3 accounts for only 10.8% of the total variance, the identification of these sources is subject to relatively high uncertainty. Consequently, PC3 represents a minor contribution to the overall PAH and N/OPAH pollution in this area compared with PC1 and PC2.

3.4. Cumulative inhalation cancer risks

The BaP_{eq} concentrations of Σ_{19} PAHs and Σ_8 NPAHs were calculated to estimate lifetime inhalation cancer risks at the sampling sites. The mean BaP_{eq} concentration of PAHs at the port sites (2.3 ng BaP_{eq}/m^3) was significantly higher than that at the industrial (0.12 ng BaP_{eq}/m^3, $p < 0.05$) and urban sites (0.12 ng BaP_{eq}/m^3, $p < 0.01$). The highest BaP_{eq} concentration of PAHs was observed at site P8, followed by sites P6 and P1, primarily due to the presence of highly toxic PAHs such as BaP and DaiP. Among the urban sites, sites U14 and U15 exhibited BaP_{eq} concentrations 3.3 and 3.9 times higher than the urban mean, respectively, indicating the influence of HMW PAHs likely transported from the port and industrial areas. For NPAHs, the mean BaP_{eq} concentration at the port sites (0.13 ng BaP_{eq}/m^3) was also significantly higher than at the industrial (0.0037 ng BaP_{eq}/m^3, $p < 0.05$) and urban sites (0.0033 ng BaP_{eq}/m^3, $p < 0.01$). Notably, site P7 showed a BaP_{eq} concentration 4.1 times higher than the mean of the port sites, mainly due to the dominance (94%) of 1-NPyr, a relatively toxic NPAH with a TEF of 0.1. Similarly, the urban sites U13–U15 showed elevated BaP_{eq} concentrations of NPAHs, also driven by high concentrations of 1-NPyr. The mean BaP_{eq} concentration of PAHs at the port sites was higher than those observed in industrial areas of Ulsan, South Korea (1.1 ng BaP_{eq}/m^3) (Vuong et al., 2020), Dongjiakou, China (0.66 ng BaP_{eq}/m^3) (Wang et al., 2022), and heavily trafficked sites in Hamadan, Iran (0.35 ng BaP_{eq}/m^3) (Nadali et al., 2021), but lower than the urban level reported in Beijing, China (3.0 ng BaP_{eq}/m^3) (Jin et al., 2017). For NPAHs, BaP_{eq} concentrations at the port sites exceeded those reported in the industrial areas of Dongjiakou, China (0.0011 ng BaP_{eq}/m^3) (Wang et al., 2022), residential sites in Xi'an, China (0.040 ng BaP_{eq}/m^3) (Wang et al., 2017), and industrial areas of Taiyuan, China (0.032 ng BaP_{eq}/m^3) (Li et al., 2014).

Cancer risks were expressed as percentiles ranging from the 5th to the 95th, in 10 intervals. The spatial distributions of mean cancer risks for PAHs and NPAHs are illustrated in Fig. 6. Using the IDW method, risk values from all sampling sites were interpolated to create risk maps based on 500 m × 500 m grid cells, which were then compared with the population map (Fig. S9). The mean cancer risks for PAHs and NPAHs were estimated as 1.62×10^{-7} and 8.55×10^{-9}, respectively. The

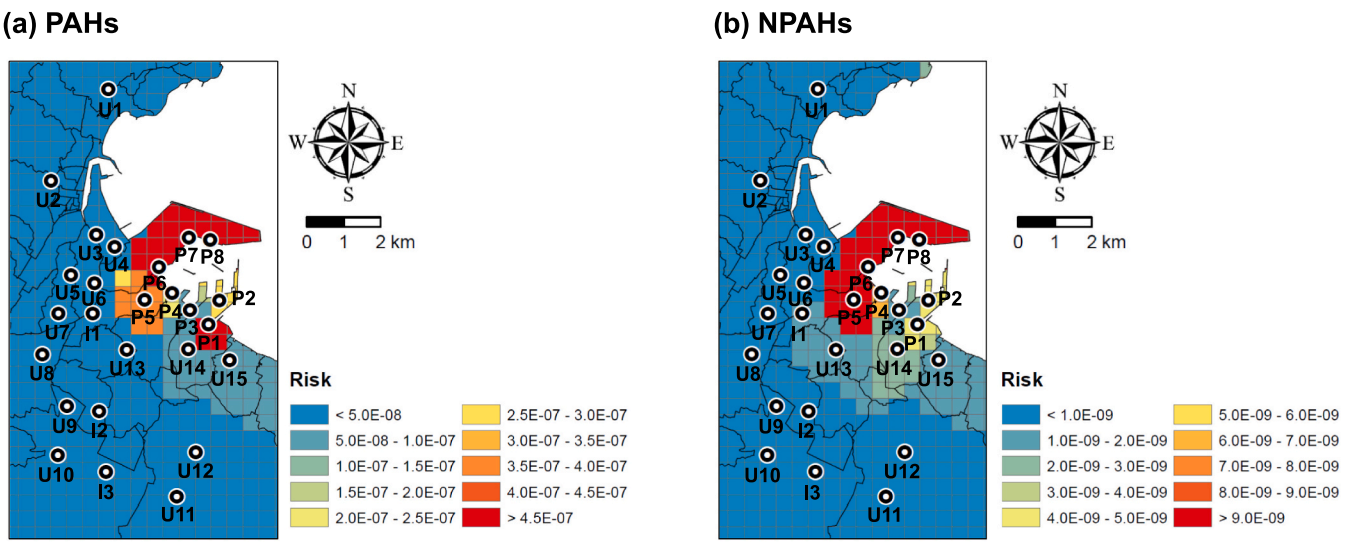

Fig. 6. Spatial distributions of the cumulative inhalation cancer risk derived from the BaP_{eq} concentrations of (a) PAHs and (b) NPAHs.

highest mean cancer risks were observed at the port sites (PAHs: 4.72×10^{-7}, NPAHs: 2.62×10^{-8}), followed by the industrial sites (PAHs: 2.45×10^{-8}, NPAHs: 7.8×10^{-10}) and the urban sites (PAHs: 2.41×10^{-8}, NPAHs: 7.01×10^{-10}). Cancer risks below 1×10^{-6} (one additional case per million people) are generally not of concern, whereas risks exceeding 1×10^{-4} are considered unacceptable. Cancer risks between 1×10^{-6} and 1×10^{-4} fall within the acceptable range (US EPA, 2020). Notably, all sampling sites in Pohang exhibited cancer risks below the 1×10^{-6} threshold. The maximum cancer risk for PAHs (8.91×10^{-7}) was recorded at site P8, while the highest risk for NPAHs (1.09×10^{-7}) was observed at site P7, consistent with elevated concentrations of these compounds. At the industrial sites, the mean PAH-related cancer risk exceeded the overall mean, while NPAH-related risks remained low, indicating that PAHs are the dominant contributor to cancer risk. Among the urban sites, U11 and U12 had lower mean cancer risks for PAHs (8.01×10^{-9}) and NPAHs (4.74×10^{-10}) compared with sites U13 to U15, where the mean risks were 6.61×10^{-8} for PAHs and 1.68×10^{-9} for NPAHs. However, the higher population density at U11 and U12 may lead to greater population exposure, especially during winter when westerly winds transport air pollutants from the industrial complex. Likewise, western residential areas (U1–U8) may be affected during summer due to pollutant transport from the port area via prevailing northeasterly winds. In particular, PM-bound toxic PAHs and NPAHs emitted from iron and steel manufacturing at the western port sites may be transported into nearby residential areas, thereby increasing cancer risks for local populations.

In summary, emissions of NPAHs from iron and steel production near the port area likely exceed those from other sources, contributing to the elevated BaP_{eq} concentrations observed in this study. Based on TEF values, most NPAHs are more toxic than their parent PAHs; for example, 6-NChr is 1000 times more toxic than Chr. Although BaP_{eq} values of NPAHs were considerably lower than those of PAHs, their greater toxicity highlights the need for cumulative risk assessment, defined as the analysis, characterization, and quantification of the combined risks posed by multiple agents (US EPA, 2003). These elevated levels may pose greater risks to vulnerable subpopulations, such as children, older adults, and those individuals with pre-existing respiratory conditions, who are more susceptible to systemic toxicity from industrial emissions. While several studies have investigated the toxicity of PAH derivatives (Durant et al., 1996; Elzein et al., 2019; Vuong et al., 2020), the toxicological characteristics of most compounds remain poorly understood. Further toxicological studies are needed to clarify the health effects of PAHs and their derivatives.

4. Conclusion

The levels, spatial distribution, sources, and health risks of PAHs, NPAHs, and OPAHs in Pohang, South Korea, were investigated using PASs deployed at 26 sites across port, industrial, and urban areas. PAH and N/OPAH concentrations were significantly higher in the port area, particularly at Piers 1 and 2, primarily due to iron ore and coal handling, iron and steel production, and vehicular emissions. Adjacent urban areas were also strongly influenced by industrial and port-related emissions, likely intensified by prevailing winds. Correlation analysis and diagnostic ratios indicated contributions from both primary sources (e.g., diesel exhaust and industrial activities) and secondary formation, with the latter playing a larger role in the urban areas. PCA identified three major sources: secondary formation (PC1, 38%), which was predominant in the urban areas; primary emissions from industry and traffic (PC2, 19.5%), concentrated in the port area; and mixed sources (PC3, 10.8%), distributed across all areas. Cancer risk assessments showed elevated risks in the port area; however, the levels remained below the threshold of concern.

Nevertheless, the potential health impacts of long-term exposure to PAHs and their derivatives, particularly in densely populated urban areas downwind of the port and the industrial complex, require continued attention. Currently, ambient air quality standards for PAHs are lacking in South Korea, and emission standards for stationary sources are limited to BaP. Even when large-scale facilities comply with BaP emission limits, emissions of a broad range of PAHs and their derivatives remain a concern. To effectively manage air quality in high-risk areas, regulatory frameworks may need to move toward TEQ-based standards encompassing these compounds. Given the current regulatory gaps, the results of this study highlight the importance of including PAH derivatives, such as NPAHs and OPAHs, in routine air quality monitoring and risk assessment, particularly in residential areas near ports and industrial facilities. Future research should focus on the toxicological effects and formation mechanisms of N/OPAHs to improve understanding of their health implications and environmental fate.

CRediT authorship contribution statement

Minji Go: Writing – original draft, Formal analysis, Conceptualization. **Ho-Young Lee:** Formal analysis. **Jeong-Tae Ju:** Formal analysis. **Seongjin Hong:** Project administration. **Sung-Deuk Choi:** Writing – review & editing, Supervision, Project administration.

Declaration of competing interest

The authors declare that they have no known competing financial interests or personal relationships that could have appeared to influence the work reported in this paper.

Acknowledgements

This study was supported by the Korea Institute of Marine Science & Technology Promotion (KIMST-20220534). Additional support was provided by the Basic Science Research Program through the National Research Foundation of Korea, funded by the Ministry of Education (RS-2020-NR049578).

Appendix A. Supplementary data

Supplementary data to this article can be found online at https://doi.org/10.1016/j.marpolbul.2026.119817.

Data availability

Data will be made available on request.

References

Albinet, A., Leoz-Garziandia, E., Budzinski, H., Villenave, E., 2007. Polycyclic aromatic hydrocarbons (PAHs), nitrated PAHs and oxygenated PAHs in ambient air of the Marseilles area (south of France): concentrations and sources. Sci. Total Environ. 384, 280–292.

Arey, J., Zielinska, B., Atkinson, R., Winer, A.M., Ramdahl, T., Pitts Jr., J.N., 1986. The formation of nitro-PAH from the gas-phase reactions of fluoranthene and pyrene with the OH radical in the presence of NO_X. Atmos. Environ. 20, 2339–2345.

Baek, K.-M., Kim, M.-J., Kim, J.-Y., Seo, Y.-K., Baek, S.-O., 2020. Characterization and health impact assessment of hazardous air pollutants in residential areas near a large iron-steel industrial complex in Korea. Atmos. Pollut. Res. 11, 1754–1766.

Bandowe, B.A.M., Meusel, H., 2017. Nitrated polycyclic aromatic hydrocarbons (nitro-PAHs) in the environment – a review. Sci. Total Environ. 581-582, 237–257.

Cave, M.R., Wragg, J., Beriro, D.J., Vane, C., Thomas, R., Riding, M., Taylor, C., 2018. An overview of research and development themes in the measurement and occurrences of polyaromatic hydrocarbons in dusts and particulates. J. Hazard. Mater. 360, 373–390.

Chen, L., Liu, W., Tao, S., Liu, W., 2021. Spatiotemporal variations and source identification of atmospheric nitrated and oxygenated polycyclic aromatic hydrocarbons in the coastal cities of the Bohai and yellow seas in northern China. Chemosphere 279, 130565.

Choi, S.-D., Kwon, H.-O., Lee, Y.-S., Park, E.-J., Oh, J.-Y., 2012. Improving the spatial resolution of atmospheric polycyclic aromatic hydrocarbons using passive air samplers in a multi-industrial city. J. Hazard. Mater. 241, 252–258.

Ciccioli, P., Cecinato, A., Brancaleoni, E., Frattoni, M., Zacchei, P., Miguel, A.H., de Castro Vasconcellos, P., 1996. Formation and transport of 2-nitrofluoranthene and 2-nitropyrene of photochemical origin in the troposphere. J. Geophys. Res. Atmos. 101, 19567–19581.

Ding, Z., Yi, Y., Zhang, Q., Zhuang, T., 2019. Theoretical investigation on atmospheric oxidation of fluorene initiated by OH radical. Sci. Total Environ. 669, 920–929.

Durant, J.L., Busby, W.F., Lafleur, A.L., Penman, B.W., Crespi, C.L., 1996. Human cell mutagenicity of oxygenated, nitrated and unsubstituted polycyclic aromatic hydrocarbons associated with urban aerosols. Mutat. Res. Genet. Toxicol. Environ. Mutagen. 371, 123–157.

Elzein, A., Dunmore, R.E., Ward, M.W., Hamilton, J.F., Lewis, A.C., 2019. Variability of polycyclic aromatic hydrocarbons and their oxidative derivatives in wintertime Beijing, China. Atmos. Chem. Phys. 19, 8741–8758.

Harner, T., Su, K., Genualdi, S., Karpowicz, J., Ahrens, L., Mihele, C., Schuster, J., Charland, J.-P., Narayan, J., 2013. Calibration and application of PUF disk passive air samplers for tracking polycyclic aromatic compounds (PACs). Atmos. Environ. 75, 123–128.

He, J., Balasubramanian, R., 2010. A comparative evaluation of passive and active samplers for measurements of gaseous semi-volatile organic compounds in the tropical atmosphere. Atmos. Environ. 44, 884–891.

Hong, Y., Xu, X., Liao, D., Ji, X., Hong, Z., Chen, Y., Xu, L., Li, M., Wang, H., Zhang, H., 2021. Air pollution increases human health risks of $PM_{2.5}$-bound PAHs and nitro-PAHs in the Yangtze River Delta, China. Sci. Total Environ. 770, 145402.

Huang, B., Liu, M., Bi, X., Chaemfa, C., Ren, Z., Wang, X., Sheng, G., Fu, J., 2014. Phase distribution, sources and risk assessment of PAHs, NPAHs and OPAHs in a rural site of Pearl River Delta region, China. Atmos. Pollut. Res. 5, 210–218.

IARC, 2010. Ingested Nitrate and Nitrite, and Cyanobacterial Peptide Toxins 94. International Agency for Research on Cancer (IARC).

IARC, 2013. Diesel and Gasoline Engine Exhausts and Some Nitroarenes 105. International Agency for Research on Cancer (IARC).

Idowu, O., Semple, K.T., Ramadass, K., O'Connor, W., Hansbro, P., Thavamani, P., 2020. Analysis of polycyclic aromatic hydrocarbons (PAHs) and their polar derivatives in soils of an industrial heritage city of Australia. Sci. Total Environ. 699, 134303.

Jariyasopit, N., Zhang, Y., Martin, J.W., Harner, T., 2018. Comparison of polycyclic aromatic compounds in air measured by conventional passive air samplers and passive dry deposition samplers and contributions from petcoke and oil sands ore. Atmos. Chem. Phys. 18, 9161–9171.

Jia, J., Cheng, S., Yao, S., Xu, T., Zhang, T., Ma, Y., Wang, H., Duan, W., 2018. Emission characteristics and chemical components of size-segregated particulate matter in iron and steel industry. Atmos. Environ. 182, 115–127.

Jin, R., Liu, G., Jiang, X., Liang, Y., Fiedler, H., Yang, L., Zhu, Q., Xu, Y., Gao, L., Su, G., 2017. Profiles, sources and potential exposures of parent, chlorinated and brominated polycyclic aromatic hydrocarbons in haze associated atmosphere. Sci. Total Environ. 593, 390–398.

Kim, S.-J., Lee, S.-J., Lee, H.-Y., Park, H.-J., Kim, C.-H., Lim, H.-J., Lee, S.-B., Kim, J.Y., Schlink, U., Choi, S.-D., 2021. Spatial-seasonal variations and source identification of volatile organic compounds using passive air samplers in the metropolitan city of Seoul, South Korea. Atmos. Environ. 246, 118136.

Kim, S.-J., Lee, H.-Y., Lee, S.-J., Choi, S.-D., 2023. Passive air sampling of VOCs, O_3, NO_2, and SO_2 in the large industrial city of Ulsan, South Korea: spatial–temporal variations, source identification, and ozone formation potential. Environ. Sci. Pollut. Res. 30, 125478–125491.

Lee, H.H., Choi, N.R., Lim, H.B., Yi, S.M., Kim, Y.P., Lee, J.Y., 2018. Characteristics of oxygenated PAHs in PM_{10} at Seoul, Korea. Atmos. Pollut. Res. 9, 112–118.

Li, R.-J., Kou, X.-J., Geng, H., Dong, C., Cai, Z.-W., 2014. Pollution characteristics of ambient $PM_{2.5}$-bound PAHs and NPAHs in a typical winter time period in Taiyuan. Chin. Chen. Lett. 25, 663–666.

Li, Y., Yang, L., Chen, X., Jiang, P., Gao, Y., Zhang, J., Yu, H., Wang, W., 2018. Indoor/outdoor relationships, sources and cancer risk assessment of NPAHs and OPAHs in $PM_{2.5}$ at urban and suburban hotels in Jinan, China. Atmos. Environ. 182, 325–334.

Lim, L.H., Harrison, R.M., Harrad, S., 1999. The contribution of traffic to atmospheric concentrations of polycyclic aromatic hydrocarbons. Environ. Sci. Technol. 33, 3538–3542.

Liu, D., Lin, T., Syed, J.H., Cheng, Z., Xu, Y., Li, K., Zhang, G., Li, J., 2017. Concentration, source identification, and exposure risk assessment of $PM_{2.5}$-bound parent PAHs and nitro-PAHs in atmosphere from typical Chinese cities. Sci. Rep. 7, 10398.

Liu, P., Ju, Y., Li, Y., Wang, Z., Mao, X., Cao, H., Jia, C., Huang, T., Gao, H., Ma, J., 2019. Spatiotemporal variation of atmospheric nitrated polycyclic aromatic hydrocarbons in semi-arid and petrochemical industrialized Lanzhou City, Northwest China. Environ. Sci. Pollut. Res. 26, 1857–1870.

Marquès, M., Mari, M., Sierra, J., Nadal, M., Domingo, J.L., 2017. Solar radiation as a swift pathway for PAH photodegradation: a field study. Sci. Total Environ. 581, 530–540.

McWhinney, R.D., Zhou, S., Abbatt, J.P.D., 2013. Naphthalene SOA: redox activity and naphthoquinone gas–particle partitioning. Atmos. Chem. Phys. 13, 9731–9744.

Meng, Y., Liu, X., Lu, S., Zhang, T., Jin, B., Wang, Q., Tang, Z., Liu, Y., Guo, X., Zhou, J., 2019. A review on occurrence and risk of polycyclic aromatic hydrocarbons (PAHs) in lakes of China. Sci. Total Environ. 651, 2497–2506.

MOE, 2023. Annual Report of Air Quality, 2022 (in Korean). Ministry of Environment of the Republic of Korea.

Nadali, A., Leili, M., Bahrami, A., Karami, M., Afkhami, A., 2021. Phase distribution and risk assessment of PAHs in ambient air of Hamadan. Iran. Ecotoxicol. Environ. Safe. 209, 111807.

Nagato, E.G., 2018. PAHs and NPAHs in airborne particulate matter: initial formation and atmospheric transformations. In: Hayakawa, K. (Ed.), Polycyclic Aromatic Hydrocarbons: Environmental Behavior and Toxicity in East Asia. Springer, Singapore, pp. 11–25.

Nguyen, T.N.T., Kwon, H.-O., Lammel, G., Jung, K.-S., Lee, S.-J., Choi, S.-D., 2020. Spatially high-resolved monitoring and risk assessment of polycyclic aromatic hydrocarbons in an industrial city. J. Hazard. Mater. 393, 122409.

de Oliveira Galvão, M.F., Scaramboni, C., Ünlü Endirlik, B., Vieira Silva, A., Öberg, M., Pozza, S.A., Watanabe, T., de Oliveira Rodrigues, P.C., de Castro Vasconcellos, P., Sadiktsis, I., Dreij, K., 2024. Application of an in vitro new approach methodology to determine relative cancer potency factors of air pollutants based on whole mixtures. Environ. Int. 190, 108942.

Reisen, F., Arey, J., 2005. Atmospheric reactions influence seasonal PAH and nitro-PAH concentrations in the Los Angeles basin. Environ. Sci. Technol. 39, 64–73.

Ringuet, J., Leoz-Garziandia, E., Budzinski, H., Villenave, E., Albinet, A., 2012. Particle size distribution of nitrated and oxygenated polycyclic aromatic hydrocarbons (NPAHs and OPAHs) on traffic and suburban sites of a European megacity: Paris (France). Atmos. Chem. Phys. 12, 8877–8887.

Ryu, H.-s., Ha, J.C., Chung, I., Yang, S., Kim, H., Choi, S.-D., 2023. Particulate matter concentration effects on attention to environmental issues: a cross-sectional study among residents in Korea's Pohang Industrial Complex. Ann. Occup. Environ. Med. 35.

Sari Doré, F., Carstens, C., Top, J., Zhang, Y., Dubois, C., Perrier, S., El Haddad, I., Bell, D. M., Riva, M., 2025. Photodegradation of naphthalene-derived particle oxidation products. Environ. Sci.: Atmos. 5, 300–315.

Shen, G., Tao, S., Wang, W., Yang, Y., Ding, J., Xue, M., Min, Y., Zhu, C., Shen, H., Li, W., 2011. Emission of oxygenated polycyclic aromatic hydrocarbons from indoor solid fuel combustion. Environ. Sci. Technol. 45, 3459–3465.

Shen, G., Tao, S., Wei, S., Zhang, Y., Wang, R., Wang, B., Li, W., Shen, H., Huang, Y., Chen, Y., 2012. Emissions of parent, nitro, and oxygenated polycyclic aromatic hydrocarbons from residential wood combustion in rural China. Environ. Sci. Technol. 46, 8123–8130.

Shen, G., Tao, S., Wei, S., Chen, Y., Zhang, Y., Shen, H., Huang, Y., Zhu, D., Yuan, C., Wang, H., 2013. Field measurement of emission factors of PM, EC, OC, parent, nitro-, and oxy-polycyclic aromatic hydrocarbons for residential briquette, coal cake, and wood in rural Shanxi, China. Environ. Sci. Technol. 47, 2998–3005.

Shin, S.M., Lee, J.Y., Shin, H.J., Kim, Y.P., 2022. Seasonal variation and source apportionment of oxygenated polycyclic aromatic hydrocarbons (OPAHs) and polycyclic aromatic hydrocarbons (PAHs) in $PM_{2.5}$ in Seoul, Korea. Atmos. Environ. 272, 118937.

Shoeib, M., Harner, T., 2002. Characterization and comparison of three passive air samplers for persistent organic pollutants. Environ. Sci. Technol. 36, 4142–4151.

Tang, N., Hattori, T., Taga, R., Igarashi, K., Yang, X., Tamura, K., Kakimoto, H., Mishukov, V.F., Toriba, A., Kizu, R., 2005. Polycyclic aromatic hydrocarbons and nitropolycyclic aromatic hydrocarbons in urban air particulates and their relationship to emission sources in the Pan–Japan Sea countries. Atmos. Environ. 39, 5817–5826.

Tang, N., Tokuda, T., Izzaki, A., Tamura, K., Ji, R., Zhang, X., Dong, L., Kameda, T., Toriba, A., Hayakawa, K., 2011. Recent changes in atmospheric polycyclic aromatic hydrocarbons (PAHs) and nitropolycyclic aromatic hydrocarbons (NPAHs) in Shenyang, China. Environ. Forensic 12, 342–348.

Teixeira, E.C., Garcia, K.O., Meincke, L., Leal, K.A., 2011. Study of nitro-polycyclic aromatic hydrocarbons in fine and coarse atmospheric particles. Atmos. Res. 101, 631–639.

Thang, P.Q., Kim, S.-J., Lee, S.-J., Kim, C.H., Lim, H.-J., Lee, S.-B., Kim, J.Y., Vuong, Q.T., Choi, S.-D., 2020. Monitoring of polycyclic aromatic hydrocarbons using passive air samplers in Seoul, South Korea: spatial distribution, seasonal variation, and source identification. Atmos. Environ. 229, 117460.

Tsapakis, M., Stephanou, E.G., 2005. Polycyclic aromatic hydrocarbons in the atmosphere of the eastern Mediterranean. Environ. Sci. Technol. 39, 6584–6590.

Tutino, M., Di Gilio, A., Laricchiuta, A., Assennato, G., de Gennaro, G., 2016. An improved method to determine PM-bound nitro-PAHs in ambient air. Chemosphere 161, 463–469.

US EPA, 1995. Compilation of Air Pollutant Emission Factors. Volume I: Stationary Point and Area Sources. United States Environmental Protection Agency (US EPA).

US EPA, 2003. Framework for Cumulative Risk Assessment. United States Environmental Protection Agency (US EPA).

US EPA, 2020. RCRA Delisting Technical Support Document (Chapter 4: Risk and Hazard Assessment). United States Environmental Protection Agency (US EPA).

Vuong, Q.T., Kim, S.-J., Nguyen, T.N.T., Thang, P.Q., Lee, S.-J., Ohura, T., Choi, S.-D., 2020. Passive air sampling of halogenated polycyclic aromatic hydrocarbons in the largest industrial city in Korea: spatial distributions and source identification. J. Hazard. Mater. 382, 121238.

Wang, J., Xu, H., Guinot, B., Li, L., Ho, S.S.H., Liu, S., Li, X., Cao, J., 2017. Concentrations, sources and health effects of parent, oxygenated-and nitrated-polycyclic aromatic hydrocarbons (PAHs) in middle-school air in Xi'an, China. Atmos. Res. 192, 1–10.

Wang, P., Qi, A., Huang, Q., Wang, Y., Tuo, X., Zhao, T., Duan, S., Gao, H., Zhang, W., Xu, P., 2022. Spatial and temporal variation, source identification, and toxicity evaluation of brominated/chlorinated/nitrated/oxygenated-PAHs at a heavily industrialized area in eastern China. Sci. Total Environ. 822, 153542.

Wei, L., Yu, Z., Zhu, C., Chen, Y., Pei, Z., Li, Y., Yang, R., Zhang, Q., Jiang, G., 2023. An evaluation of the impact of traffic on the distribution of PAHs and oxygenated PAHs in the soils and moss of the southeast Tibetan plateau. Sci. Total Environ. 862, 160938.

Wei, S., Huang, B., Liu, M., Bi, X., Ren, Z., Sheng, G., Fu, J., 2012. Characterization of $PM_{2.5}$-bound nitrated and oxygenated PAHs in two industrial sites of South China. Atmos. Res. 109, 76–83.

Zhang, J., Yang, L., Ledoux, F., Courcot, D., Mellouki, A., Gao, Y., Jiang, P., Li, Y., Wang, W., 2019. $PM_{2.5}$-bound polycyclic aromatic hydrocarbons (PAHs) and nitrated PAHs (NPAHs) in rural and suburban areas in Shandong and Henan provinces during the 2016 Chinese New Year's holiday. Environ. Pollut. 250, 782–791.

Zhang, L., Yang, L., Zhou, Q., Zhang, X., Xing, W., Wei, Y., Hu, M., Zhao, L., Toriba, A., Hayakawa, K., 2020. Size distribution of particulate polycyclic aromatic hydrocarbons in fresh combustion smoke and ambient air: a review. J. Environ. Sci. 88, 370–384.

Zhuo, S., Du, W., Shen, G., Li, B., Liu, J., Cheng, H., Xing, B., Tao, S., 2017. Estimating relative contributions of primary and secondary sources of ambient nitrated and oxygenated polycyclic aromatic hydrocarbons. Atmos. Environ. 159, 126–134.